Phase Boundaries of CO_2 + Toluene, CO_2 + Acetone, and CO_2 + Ethanol at High Temperatures and High Pressures

Weize Wu, Jie Ke, and Martyn Poliakoff*

The School of Chemistry, The University of Nottingham, Nottingham NG7 2RD, U.K.

The phase boundaries of the CO_2 + toluene, CO_2 + acetone, and CO_2 + ethanol binary systems have been measured via a dynamic synthetic method based on a fiber optic reflectometer. We focus on a wide range of concentration of CO_2 from 0.2 to 0.9 in mole fraction with temperatures up to 572 K. The results are correlated by the Peng−Robinson equation of state (PR-EOS) with two interaction parameters, which shows that the PR-EOS can predict the phase boundaries of CO_2 + toluene and CO_2 + acetone well but cannot predict the phase boundaries of the CO_2 + ethanol binary system.

Introduction

Phase behavior is of technological interest for the design, development, and operation of many chemical processes and separations that are conducted at high pressures and high temperatures, especially for supercritical fluid processes, where phase behavior can significantly influence the reaction rate, selectivity, mass transfer properties, etc.[1−3] Therefore, phase behavior has been studied over many years, and numerous methods have been developed for measuring the phase behavior of fluid mixtures. Several review articles on high-pressure fluid phase behavior, experimental methods, and systems have been published.[4−6]

Carbon dioxide is one of the more popular solvents because it is nontoxic, nonflammable, inexpensive, readily available in large quantities, and has moderate critical temperature and pressure (304.3 K and 7.38 MPa). Supercritical carbon dioxide is recognized as an environmentally benign solvent, and it has been widely used as the solvent in supercritical fluid extraction and chemical reactions. Toluene, acetone, and ethanol are common solvents used in the chemical and polymer industry; they are also commonly used as cosolvents to modify the properties of supercritical CO_2 or as anti-solvents for material synthesis.

The phase behavior of CO_2 and toluene, acetone, or ethanol have been studied by several groups. Initially, Ng and Robinson[7] and Sebastian et al.[8] measured the isothermal phase boundaries of CO_2 and toluene at temperatures up to 477 K and 543 K, respectively. Kim et al.[9] and Tochigi et al.[10] investigated the same system at low temperatures up to 392.2 K and 333.15 K, respectively. Recently, Lazzaroni et al.[11] reported phase behavior of CO_2 + toluene and CO_2 + acetone systems at 323.2 K. Giacobbe[12] measured the solubility of CO_2 in acetone at temperatures of 293.15 and 303.15 K. Katayama et al.[13] obtained the vapor−liquid equilibrium data at temperatures of 298.15 K and 313.15 K up to 8 MPa for CO_2 + acetone mixtures. Chang and co-workers[14,15] determined the phase diagram for CO_2 + acetone and CO_2 + ethanol mixtures at temperatures from 291.15 K to 313.15 K up to 8 MPa. The phase behavior of CO_2 + ethanol has also been measured at temperatures not more than 337 K by several authors.[16−19] Galicia-Luna and Ortega-Rodriguez[20] reported phase equilibrium data of the same system at higher temperatures up to 373 K using a static analytic method.

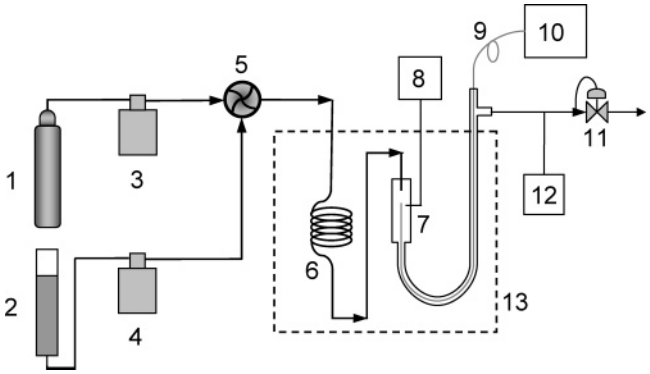

Figure 1. Schematic diagram of the apparatus for measuring phase boundary of mixed fluids at high temperatures and high pressures: 1, CO_2 cylinder; 2, metrical cylinder; 3, CO_2 pump; 4, liquid solvent pump; 5, mixer; 6, preheater; 7, equilibrium cell; 8, digital temperature monitor; 9, optic fiber; 10, personal computer; 11, back pressure regulator; 12, pressure gauge; 13, temperature controlled oven (dotted line).

Most of these studies were focused on the phase behavior at relatively low temperatures. There is a shortage of phase behavior data at higher temperatures because of the limitations of the apparatus at these temperatures. However, high temperatures and pressures are essential for important chemical processes, such as oxidation, hydrogenation, and hydroformylation in supercritical fluids.[21,22]

In this paper, we use our newly developed dynamic synthetic method based on a fiber optic reflectometer (FOR)[23] to measure the phase behavior of CO_2 + toluene, CO_2 + acetone, and CO_2 + ethanol with concentrations of organic solvent up to 80 mol %. The data are correlated with the Peng−Robinson cubic equation of state (PR-EOS) with the van der Waals mixing rules.[24]

Experimental Section

Materials. CO_2 (99.95 %) was purchased from BOC Gases. Acetone (99.98 %), toluene (99.99 %), and ethanol (99.98 %)

* Corresponding author. E-mail: Martyn.Poliakoff@nottingham.ac.uk. Tel.: +44 115 951 3520. Fax: +44 115 951 3058.

10.1021/je060099a CCC: $33.50
Published on Web 06/17/2006

Table 1. Phase Boundaries of CO_2 (1) and Toluene (2) at Different Conditions

T/K	p/MPa	phase transition[a]	T/K	p/MPa	phase transition[a]	T/K	p/MPa	phase transition[a]	T/K	p/MPa	phase transition[a]
						$x_2 = 0.10$					
333.2	10.16	cp	373.2	13.74	d	403.2	13.57	d	427.4	8.62	d
343.2	11.27	d	383.2	13.98	d	420.5	12.43	d	426.8	7.67	d
353.2	12.29	d	393.2	13.98	d	424.5	10.60	d	425.3	6.77	d
363.2	13.11	d									
						$x_2 = 0.20$					
333.2	9.47	b	383.2	14.86	b	423.2	15.99	d	468.7	12.42	d
343.2	10.93	b	393.2	15.51	cp	433.2	15.71	d	472.2	10.65	d
353.2	12.03	b	403.2	15.86	d	443.2	15.07	d	473.2	8.62	d
363.2	13.18	b	413.2	15.99	d	451.0	14.34	d	466.8	6.79	d
373.2	14.11	b									
						$x_2 = 0.30$					
333.2	8.83	b	393.2	15.28	b	453.2	16.34	d	501	10.60	d
343.2	10.05	b	403.2	15.96	b	463.2	15.82	d	502	9.67	d
353.2	11.28	b	413.2	16.30	b	473.2	15.10	d	502	8.62	d
363.2	12.42	b	423.2	16.49	b	483	13.88	d	499	7.69	d
373.2	13.62	b	433.2	16.58	d	494	12.46	d	496	6.77	d
383.2	14.55	b	443.2	16.49	d	497	11.54	d			
						$x_2 = 0.40$					
333.2	8.09	b	393.2	13.97	b	453.2	16.35	b	504	13.37	d
343.2	8.91	b	403.2	14.81	b	463.2	16.08	b	510	12.44	d
353.2	10.16	b	413.2	15.46	b	473.2	15.69	d	521	10.60	d
363.2	11.20	b	423.2	15.92	b	483	15.17	d	522	8.65	d
373.2	12.12	b	433.2	16.19	b	493	14.40	d	516	6.79	d
383.2	13.14	b	443.2	16.35	b						
						$x_2 = 0.50$					
333.2	6.79	b	413.2	12.72	b	485	14.94	b	534	10.62	d
353.2	8.48	b	433.2	13.84	b	493	14.57	d	539	8.62	d
373.2	9.98	b	453.2	15.12	b	499	14.09	d	535	6.77	d
393.2	11.41	b	473.2	15.22	b	520	12.47	d			
						$x_2 = 0.60$					
353.2	6.99	b	433.2	11.29	b	503	12.75	b	548	9.64	d
373.2	8.20	b	453.2	11.93	b	513	12.48	b	552	8.62	d
393.2	9.47	b	473.2	12.40	b	523	12.01	b	550	6.77	d
413.2	10.35	b	493	12.80	b	533	11.19	b			
						$x_2 = 0.70$					
393.2	7.36	b	453.2	9.49	b	513	10.39	b	557	8.60	d
413.2	8.01	b	473.2	10.01	b	533	10.31	b	563	7.69	d
433.2	8.85	b	493	10.21	b	553	9.02	d	564	6.77	d
						$x_2 = 0.80$					
493	6.83	b	533	7.62	b	565	7.20	b			
513	7.47	b	553	7.67	b	572	6.74	b			

[a] Key: b, bubble point; cp, estimated critical point; d, dew point.

Table 2. Phase Boundaries of CO_2 (1) and Acetone (2) at Different Conditions

T/K	p/MPa	phase transition[a]	T/K	p/MPa	phase transition[a]	T/K	p/MPa	phase transition[a]	T/K	p/MPa	phase transition[a]
						$x_2 = 0.10$					
333.2	9.44	b	353.2	10.22	d	363.3	8.62	d	363.1	6.77	d
343.2	10.04	d	363.2	9.47	d	363.6	7.70	d			
						$x_2 = 0.20$					
333.2	8.44	b	363.2	11.18	b	393.2	10.95	b	399.9	8.61	d
343.2	9.47	b	373.2	11.51	d	397.2	10.48	d	399.2	7.69	d
353.2	10.54	b	383.2	11.51	d	399.0	9.67	d	398.3	6.77	d
						$x_2 = 0.30$					
333.2	7.14	b	373.2	10.99	b	413.2	11.51	d	425.7	8.56	d
343.2	8.06	b	383.2	11.53	b	422.5	10.59	d	425.7	7.64	d
353.2	9.17	b	393.2	11.79	b	425.9	9.60	d	423.2	6.74	d
363.2	10.23	b	403.2	11.79	d						
						$x_2 = 0.40$					
343.2	7.05	b	383.2	10.34	b	423.2	11.37	d			
353.2	7.78	b	393.2	11.00	b	433.2	10.80	d	443.4	8.64	d
363.2	8.57	b	403.2	11.45	b	437.0	10.61	d	444.5	7.68	d
373.2	9.50	b	413.2	11.55	b	441.9	9.68	d	441.5	6.76	d
						$x_2 = 0.50$					
363.2	7.10	b	403.2	10.03	b	433.2	10.90	b	458.2	8.63	d
373.2	7.76	b	413.2	10.62	b	443.2	10.44	b	458.3	7.69	d
383.2	8.72	b	423.2	10.89	b	453.9	9.67	d	456.5	6.78	d
393.2	9.39	b									
						$x_2 = 0.60$					
383.2	6.98	b	413.2	8.72	b	443.2	9.83	b	468.1	8.62	d
393.2	7.54	b	423.2	9.29	b	453.2	9.80	b	471.2	7.72	d
403.2	8.18	b	433.2	9.66	b	463.2	9.08	d	471.7	6.78	d
						$x_2 = 0.70$					
423.2	7.25	b	453.2	8.46	b	473.2	8.18	b	482	7.25	d
433.2	7.80	b	463.2	8.63	b	480	7.70	d	482	6.77	d
443.2	8.09	b									

[a] Key: b, bubble point; d, dew point.

were analytical grade and supplied by Fisher Scientific. All chemicals were used as received.

Apparatus and Procedures. In brief, the apparatus (Figure 1) consists of a CO_2 cylinder, two high-pressure reciprocating pumps (Gilson 308), a 1.5 mL dynamic mixer (Gilson 811C), a preheater (an 8 m coil of 1/16 in. o.d. tubing), an equilibrium cell, a GC oven-controlled air bath, a back-pressure regulator (BPR) (JASCO 880-81), an optic sensor, a pressure gauge, and a temperature indicator. The reciprocating pumps were used to keep constant flow rate when the system pressure was varied. To ensure that the CO_2 pump worked well, the head of the CO_2 pump was cooled by a cooler jacket, and a syringe pump (ISCO

Table 3. Phase Boundaries of CO_2 (1) and Ethanol (2) at Different Conditions

T/K	p/MPa	phase transition[a]	T/K	p/MPa	phasetransition[a]	T/K	p/MPa	phase transition[a]	T/K	p/MPa	phase transition[a]
						$x_2 = 0.10$					
333.2	10.65	d	353.2	12.26	d	373.2	11.86	d	385.2	8.483	d
343.2	11.72	d	363.2	12.42	d	381.2	10.49	d	384.2	6.76	d
						$x_2 = 0.20$					
333.2	10.63	b	363.2	13.57	d	393.2	13.94	d	414.7	10.51	d
343.2	11.91	b	373.2	14.05	d	403.2	13.31	d	415.7	8.58	d
353.2	12.82	d	383.2	14.21	d	410.1	12.35	d	413.7	6.80	d
						$x_2 = 0.30$					
333.2	10.47	b	373.2	14.24	b	413.2	14.46		435.1	9.67	d
343.2	11.73	b	383.2	14.72	cp	423.2	13.55	d	433.7	7.67	d
353.2	12.75	b	393.2	14.83	d	430.4	12.46	d	431.4	6.74	d
363.2	13.66	b	403.2	14.83	d	433.2	11.51	d			
						$x_2 = 0.40$					
333.2	9.91	b	373.2	13.98	b	413.2	14.84	b	448.8	11.43	d
343.2	11.13	b	383.2	14.45	b	423.2	14.62	d	450.8	9.56	d
353.2	12.13	b	393.2	14.82	b	433.2	14.00	d	448.4	7.63	d
363.2	13.15	b	403.2	14.91	b	443.2	13.12	d	445.0	6.75	d
						$x_2 = 0.50$					
333.2	9.24	b	383.2	13.42	b	423.2	14.44	b	460.7	11.43	d
343.2	10.27	b	393.2	13.96	b	433.2	14.15	b	464.0	9.59	d
353.2	11.29	b	403.2	14.33	b	443.2	13.62	d	461.7	7.65	d
363.2	12.11	b	413.2	14.53	b	453.2	12.78	d	458.2	6.77	d
373.2	12.76	b									
						$x_2 = 0.60$					
333.2	7.82	b	383.2	11.53	b	433.2	13.42	b	469.3	11.47	d
343.2	8.77	b	393.2	12.13	b	443.2	13.31	b	476.2	9.64	d
353.2	9.63	b	403.2	12.58	b	453.2	12.85	b	474.2	7.68	d
363.2	10.33	b	413.2	12.96	b	463.2	12.10	d	470.3	6.77	d
373.2	11.05	b	423.2	13.31	b						
						$x_2 = 0.70$					
343.2	7.00	b	383.2	9.39	b	443.2	11.51	b	483	10.00	d
353.2	7.71	b	393.2	9.84	b	453.2	11.62	b	487	8.57	d
363.2	8.37	b	413.2	10.58	b	463.2	11.58	b	486	7.65	d
373.2	8.92	b	433.2	11.24	b	473.2	11.03	b	482	6.74	d
						$x_2 = 0.80$					
393.2	7.05	b	433.2	8.42	b	483	9.73	b	496	7.68	d
403.2	7.41	b	453.2	9.13	b	493	8.87	cp	494	6.77	d
413.2	7.78	b	473.2	9.79	b						

[a] Key: b, bubble point; cp, estimated critical point; d, dew point.

260D) was used to ensure that the feed pressure of CO_2 into the reciprocating pump was kept at 6.4 MPa, which is high enough for CO_2 to be in the liquid state. The composition of the feed mixture was determined by the relative flow rates of the two pumps. A dynamic mixer ensures that the components are uniformly mixed before they flow into the preheater. The preheater heats the fluid in the tubing to the desired temperature before entering the equilibrium cell. The equilibrium cell is made up from 1/4 in. tubing 5 cm in length. A thermocouple is introduced into the vessel through a tee-piece, so that the temperature of the system can be measured accurately. The fiber is sealed to the pressure system outside the heated zone with a standard 1/16 in. stainless steel capillary/polymer (PEEK) seal. The apparatus is connected with standard Swagelok high-pressure fittings. Experiments showed that the apparatus was very effective at achieving the temperature equilibrium at a typical total flow rate of about 1 mL·min^{-1}.

Here we use the FOR to monitor the phase transition of mixed fluids. The principle of the FOR was demonstrated in our previous report.[23] The air bath is controlled by a digital temperature controller (Eurotherm 2216L), and the temperature is measured by a type-K thermocouple. The temperature stability is better than ± 0.2 K at temperatures below 473 K and ± 1.0 K at temperatures above 473 K. The BPR is used to control the system pressure, and the pressure is monitored by the pressure gauge, which is composed of a pressure transducer (RDP Electronics, model A-105) and an indicator. Its accuracy is better than ± 0.01 MPa in the pressure range of 0 to 35 MPa. However, the uncertainties of pressure measurement are ca. 0.1 MPa because of the pressure oscillation of the BPR. The flow rates of both CO_2 and organic solution pumps were calibrated before the experiment. The deviations of the pumps are better than 3.8 %. The repeatability of phase transition pressures was better than 0.1 MPa in deviation.

In a typical experiment, CO_2 and organic solvent were pumped at a fixed ratio into the equilibrium cell via the mixer and preheater. First, the temperarure and pressure are controlled until a single phase is formed in equilibrium cell. When equilibrium is reached, the signal of FOR monitored on PC screen becomes constant with time. Then, conditions can be slowly changed to reach a phase transition point, either by changing the pressure with the BPR or by changing the temperature via the temperature controller. When the phase transition is reached, there is an obvious jump on the signal value of FOR.[25]

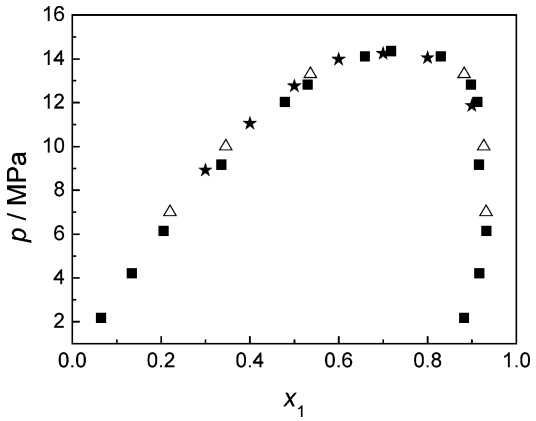

Figure 2. Experimental results for the carbon dioxide (1) + ethanol (2) system at fixed temperatures: ★, this work, at 373.2 K; ■, Galicia-Luna and Ortega-Rodriguez[20] at 373.0 K; △, Pfohl et al.[26] at 373.2 K.

Results and Discussion

The FOR method has not been reported in the literature for the phase boundary of mixed fluids. First we compared our results with the literature,[20,26] which are shown in Figure 2. The isotherms show that our results are in a good agreement with the data of the other investigators using different methods. The average absolute deviation between the measured data and the literature data is less than 2.0 %.

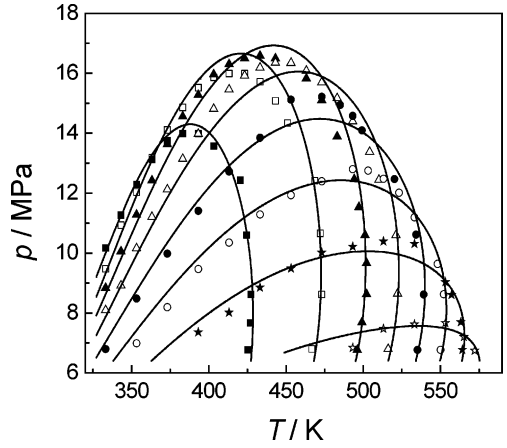

Figure 3. Phase boundaries of CO_2 (1) and toluene (2), experimental data (in symbols) calculated results by PR-EOS (in solid lines): ■, $x_2 = 0.10$; □, $x_2 = 0.20$; ▲, $x_2 = 0.30$; △, $x_2 = 0.40$; ●, $x_2 = 0.50$; ○, $x_2 = 0.60$; ★, $x_2 = 0.70$; ☆, $x_2 = 0.80$.

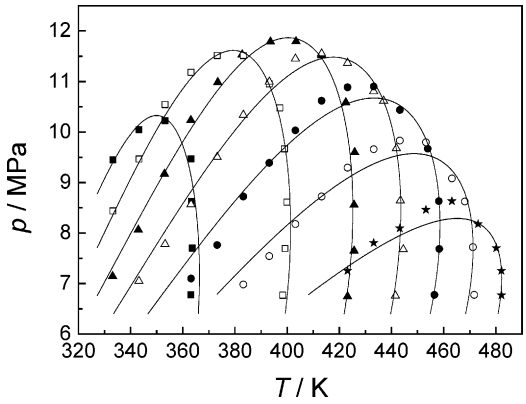

Figure 4. Phase boundaries of CO_2 (1) and acetone (1), experimental data (in symbols) and calculated results by PR-EOS (in solid lines): ■, $x_2 = 0.10$; □, $x_2 = 0.20$; ▲, $x_2 = 0.30$; △, $x_2 = 0.40$; ●, $x_2 = 0.50$; ○, $x_2 = 0.60$; ★, $x_2 = 0.70$.

Tables 1 to 3 summarize the primary experimental data of the various types of phase transition data (i.e., dew point, estimated critical point, and bubble point). Each table contains a number of different fixed overall compositions of the binary system. The mole fraction of CO_2 ranges from 0.2 to 0.9. Figures 3 to 5 give graphical representation of the experimentally determined phase boundaries. There is two-phase region below or inside lines of fixed composition, while the single-phase region is above or outside these lines.

The critical point is located between the bubble point and the dew point lines on the phase boundary. The estimated critical points for the CO_2 + toluene system are shown in Figure 6, together with literature data,[7,27] showing a good agreement between our data and theirs. The critical temperature of the mixture of CO_2 and toluene increases with increasing mole fraction of toluene, and the critical pressure of the mixture has a maximum value at a mole fraction of toluene of about 0.3. The locus of the critical points shows a continuous critical line from CO_2 critical point to toluene critical point, which covers the phase envelopes of different isopleths.

As can be seen from Figures 3 to 5, the three systems have the same qualitative shape. The three systems exhibit Type I fluid phase behavior according to the classification of six principal types of binary phase diagram,[28] which means that a continuous critical line connects the critical points of the two pure components.

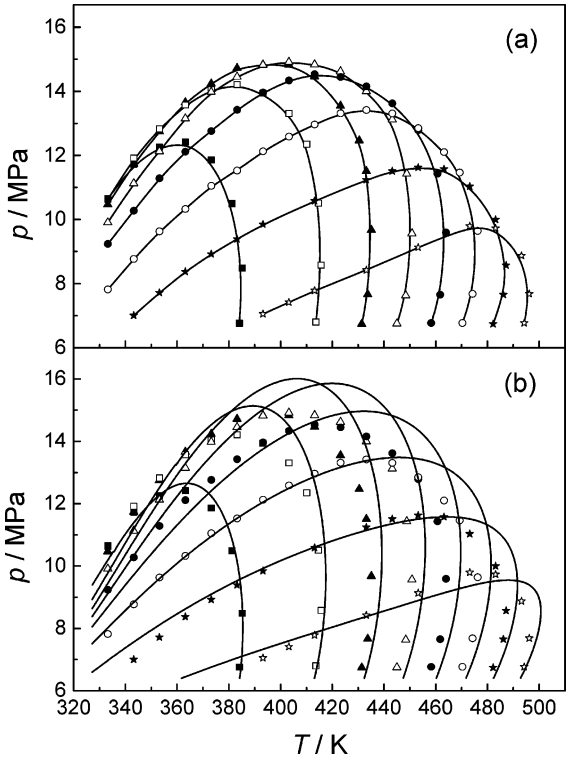

Figure 5. Phase boundaries of CO_2 (1) and ethanol (2). (a) Experimental data, (b) calculated with PR-EOS (in solid lines) to compare with experimental results (in symbols): ■, $x_2 = 0.10$; □, $x_2 = 0.20$; ▲, $x_2 = 0.30$; △, $x_2 = 0.40$; ●, $x_2 = 0.50$; ○, $x_2 = 0.60$; ★, $x_2 = 0.70$; ☆, $x_2 = 0.80$.

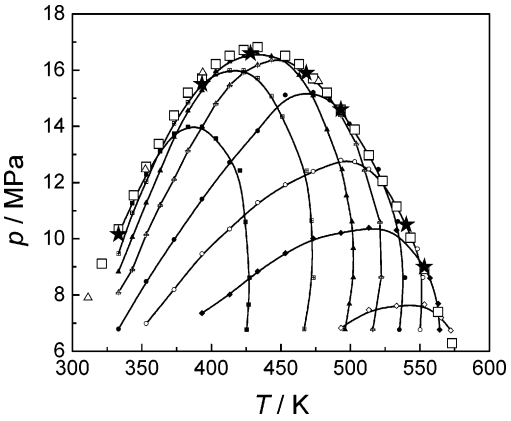

Figure 6. Critical loci and phase boundaries for CO_2 (1) and toluene (2) compared with literatures. Critical point: ★, our results (estimated); □, Ziegler et al.;[27] △, Ng and Robinson.[7] Compositions are labeled as follows in mole fraction: ■, $x_2 = 0.10$; ⊞, $x_2 = 0.20$; ▲, $x_2 = 0.30$; open triangle with cross inside, $x_2 = 0.40$; ●, $x_2 = 0.50$; ○, $x_2 = 0.60$; ◆, $x_2 = 0.70$; ◇, $x_2 = 0.80$.

Correlation of the Experimental Data. In this work, we use the Peng−Robinson cubic equation of state (PR-EOS)[24] (eq 1) to correlate the experimental data. The reasons for selecting the PR-EOS are that it requires comparatively little input information and that many of the parameters (such as interaction parameters for mixtures) are readily available in the literature for PR-EOS:

$$P = \frac{RT}{V-b} - \frac{a}{V(V+b)+b(V-b)} \tag{1}$$

For pure substances, only three parameters [T_c (critical temperature), P_c (critical pressure), and ω (acentric factor)] are

Table 4. Pure Component Parameters for Pure Fluids Used in the Peng−Robinson Equation of State

components	T_c/K	p_c/MPa	ω
CO_2	304.3	7.38	0.225
toluene	591.8	4.11	0.263
acetone	508.1	4.70	0.309
ethanol	516.2	6.38	0.635

Table 5. Interaction Parameters in the PR-EOS Simulation for CO_2 + Toluene, CO_2 + Acetone, and CO_2 + Ethanol

component *i* and *j*	k_{12}	l_{12}
CO_2 + toluene	0.060	−0.076
CO_2 + acetone	0.018	−0.065
CO_2 + ethanol	0.048	−0.079

required to calculate the parameters a and b:

$$a = 0.457235 \frac{R^2 T_c^{\,2}}{P_c} \alpha \tag{2}$$

$$b = 0.077796 \frac{RT_c}{P_c} \tag{3}$$

$$\alpha = [1 + m(1 - \sqrt{T/T_c})]^2 \tag{4}$$

$$m = 0.37464 + 1.54226\omega - 0.26992\omega^2 \tag{5}$$

For mixtures, the van der Waals mixing rule is used; a and b are calculated from the pure substance parameters by eqs 6 and 7:

$$a = \sum_i \sum_j x_i x_j \sqrt{a_i a_j}(1 - k_{ij}) \tag{6}$$

$$b = \sum_i \sum_j 0.5 x_i x_j (b_i + b_j)(1 - l_{ij}) \tag{7}$$

where x_i is the mole fraction of the ith component; a_i and b_i are the pure substance parameters defined by Peng and Robinson; and k_{ij} and l_{ij} are the binary interaction parameters for the (i, j) pair. The physical property information (T_c, P_c, and ω) used for the pure components is taken from the NIST (see Table 4).

Binary interaction parameters are empirical parameters that can be regressed from the binary data by minimizing the average absolute deviation for bubble and dew point pressures. A single interaction parameter can usually be used to calculate the phase behavior to a relatively satisfactory degree over a narrow range of temperatures.[29] In this work, however, the phase boundaries of binary mixtures are measured over a very wide range of temperatures. So two interaction parameters are needed to calculate the phase boundaries. The k_{ij} and l_{ij} values for the binary mixtures involved in this work (shown in Table 5) were obtained by minimization of errors of phase boundaries between experimental data and values calculated by the PR-EOS.

Using two interaction parameters, the PR-EOS can predict the phase boundaries of CO_2 + toluene and CO_2 + acetone to a satisfactory degree over a very wide range of temperatures from 333 K to 573 K, as shown in Figures 2 and 3. However, for the CO_2 + ethanol mixture, the PR-EOS predicts the phase boundaries to a low degree of accuracy. The reasons for this are that (i) ethanol has a much higher acentric factor than that of CO_2 (see Table 4) and (ii) ethanol can form hydrogen bonds with electron donors or acceptors and may weakly hydrogen bond with CO_2.[30,31] Although acetone (dipole moment, m = 2.89 D) is more polar than ethanol (m = 1.70 D), it cannot undergo hydrogen bonding. The hydrogen bonding is ignored when the PR-EOS calculates the phase of CO_2 and ethanol. This probably results in a substantial error for the prediction.

Conclusions

Using the synthetic dynamic method based on our FOR, we have successfully measured the phase boundaries of the binary mixtures of CO_2 + toluene, CO_2 + acetone, and CO_2 + ethanol over a wide range of concentration of CO_2 from 0.2 to 0.9 in mole fraction at temperatures up to 572 K. The phase boundary data CO_2 + toluene, CO_2 + acetone, and CO_2 + ethanol binary systems are correlated by the PR-EOS with two interaction parameters.

Acknowledgment

We thank Prof. M. W. George, Prof. M. Nunes da Ponte, Dr. P. License, Mr. M. Guyler, Mr. R. Wilson and Mr. P. Fields for their help.

Literature Cited

(1) Brennecke, J. F.; Chateauneuf, J. E. Homogeneous organic reactions as mechanistic probes in supercritical fluids. *Chem. Rev.* **1999**, *99*, 433−452.
(2) Chouchi, D.; Gourgouillon, D.; Courel, M.; Vital, J.; da Ponte, M. N. The influence of phase behavior on reactions at supercritical conditions: The hydrogenation of α-pinene. *Ind. Eng. Chem. Res.* **2001**, *40*, 2551−2554.
(3) Pereda, S.; Bottini, S. B.; Brignole, E. A. Supercritical fluids and phase behavior in heterogeneous gas−liquid catalytic reactions. *Appl. Catal. A* **2005**, *281*, 129−137.
(4) Schneider, G. M. High-pressure investigations of fluid mixtures—review and recent results. *J. Supercrit. Fluids* **1998**, *13*, 5−14.
(5) Dohrn, R.; Brunner, G. High-pressure fluid-phase equilibria—experimental methods and systems investigated (1988−1993). *Fluid Phase Equilib.* **1995**, *106*, 213−282.
(6) Christov, M.; Dohrn, R. High-pressure fluid phase equilibria—experimental methods and systems investigated (1994−1999). *Fluid Phase Equilib.* **2002**, *202*, 153−218.
(7) Ng, H. J.; Robinson, D. B. Equilibrium phase properties of toluene−carbon dioxide system. *J. Chem. Eng. Data* **1978**, *23*, 325−327.
(8) Sebastian, H. M.; Simnick, J. J.; Lin, H. M.; Chao, K. C. Gas−liquid equilibrium in mixtures of carbon dioxide plus toluene and carbon dioxide plus *m*-xylene. *J. Chem. Eng. Data* **1980**, *25*, 246−248.
(9) Kim, C.-H.; Vimalchand, P.; Donohue, M. D. Vapor−liquid equilibria for binary mixtures of carbon dioxide with benzene, toluene and *p*-xylene. *Fluid Phase Equilib.* **1986**, *31*, 299−311.
(10) Tochigi, K.; Hasegawa, K.; Asano, N.; Kojima, K. Vapor−liquid equilibria for the carbon dioxide + pentane and carbon dioxide + toluene systems. *J. Chem. Eng. Data* **1998**, *43*, 954−956.
(11) Lazzaroni, M. J.; Bush, D.; Brown, J. S.; Eckert, C. A. High-pressure vapor−liquid equilbria of some carbon dioxide + organic binary systems. *J. Chem. Eng. Data* **2005**, *50*, 60−65.
(12) Giacobbe, F. W. Thermodynamic solubility behavior of carbon dioxide in acetone. *Fluid Phase Equilib.* **1992**, *72*, 277−297.
(13) Katayama, T.; Ohgaki, K.; Maekawa, G.; Goto, M.; Nagano, T. Isothermal vapor−liquid equilibria of acetone−carbon dioxide and methanol−carbon dioxide systems at high pressures. *J. Chem. Eng. Jpn.* **1975**, *8*, 89−92.
(14) Chang, C. J.; Day, C.-Y.; Ko, C.-M.; Chiu, K.-L. Densities and $P-x-y$ diagrams for carbon dioxide dissolution in methanol, ethanol, and acetone mixtures. *Fluid Phase Equilib.* **1997**, *131*, 243−258.
(15) Day, C.-Y.; Chang, C. J.; Chen, C.-Y. Phase equilibrium of ethanol + CO_2 and acetone + CO_2 at Elevated Pressures. *J. Chem. Eng. Data* **1996**, *41*, 839−843.
(16) Suzuki, K.; Sue, H. Isothermal vapor−liquid equilibrium data for binary systems at high pressures: carbon dioxide−methanol, carbon dioxide−ethanol, carbon dioxide−1-propanol, methane−ethanol, methane−1-propanol, ethane−ethanol, and ethane−1-propanol systems. *J. Chem. Eng. Data* **1990**, *35*, 63−66.
(17) Kodama, D.; Kato, M. High-pressure phase equilibrium for carbon dioxide + ethanol at 291.15 K. *J. Chem. Eng. Data* **2005**, *50*, 16−17.
(18) Yoon, J.-H.; Lee, H.-S.; Lee, H. High-pressure vapor−liquid equilibria for carbon dioxide + methanol, carbon dioxide + ethanol, and carbon dioxide + methanol + ethanol. *J. Chem. Eng. Data* **1993**, *38*, 53−55.
(19) Jennings, D. W.; Lee, R.; Teja, A. S. Vapor−liquid equilibria in the carbon dioxide + ethanol and carbon dioxide + l-butanol systems. *J. Chem. Eng. Data* **1991**, *36*, 303−307.

(20) Galicia-Luna, L. A.; Ortega-Rodriguez, A. New apparatus for the fast determination of high-pressure vapor−liquid equilibria of mixtures and of accurate critical pressures. *J. Chem. Eng. Data* **2000**, *45*, 265−271.
(21) Jessop, P. G.; Ikariya, T.; Noyori, R. Homogeneous hydrogenation of carbon dioxide. *Chem. Rev.* **1995**, *95*, 259−272.
(22) Licence, P.; Gray, W. K.; Sokolova, M.; Gray, W. K. Selective monoprotection of 1,*n*-terminal diols in supercritical carbon dioxide: a striking example of solvent tunable desymmetrization. *J. Am. Chem. Soc.* **2005**, *127*, 293−298.
(23) Avdeev, M. V.; Konovalov, A. N.; Bagratashvili, V. N.; Popov, V. K.; Tsypina, S. I.; Sokolova, M.; Ke, J.; Poliakoff, M. The fibre optic reflectometer: a new and simple probe for refractive index and phase separation measurements in gases, liquids and supercritical fluids. *Phys. Chem. Chem. Phys.* **2004**, *6*, 1258−1263.
(24) Peng, D. Y.; Robinson, D. B. A new two-constant equation of state. *Ind. Eng. Chem. Fundam.* **1976**, *15*, 59−64.
(25) Wu, W. Z.; Ke, J.; Poliakoff, M. A new design of fiber optic reflectometer for determining the phase boundary of multi-component fluid mixtures at high pressures and high temperatures. *Rev. Sci. Instrum.* **2006**, *77*, 023903, 1−4.
(26) Pfohl, O.; Pagel, A.; Brunner, G. Phase equilibria in systems containing *o*-cresol, *p*-cresol, carbon dioxide, and ethanol at 323.15−473.15 K and 10−35 MPa. *Fluid Phase Equilib.* **1999**, *157*, 53−79.
(27) Ziegler, J. W.; Dorsey, J. G.; Chester, T. L.; Innis, D. P. Estimation of liquid−vapor critical loci for con-solvent mixtures using a peak-shape method. *Anal. Chem.* **1995**, *67*, 456−461.
(28) Scott, R. L.; van Konynenburg, P. H. Static properties of solutions. van der Waals and related models for hydrocarbon mixtures. *Discuss. Faraday Soc.* **1970**, *49*, 87−97.
(29) Ke, J.; George, M. W.; Poliakoff, M.; Han, B.; Yan, H. How does the critical point change during the hydrogenation of propene in supercritical carbon dioxide? *J. Phys. Chem. B* **2002**, *106*, 4496−4502.
(30) Raveendran, P.; Ikushima, Y.; Wallen, S. L. Polar attributes of supercritical carbon dioxide. *Acc. Chem. Res.* **2005**, *38*, 478−485.
(31) Tsivintzelis, I.; Missopolinou, D.; Kalogiannis, K.; Panayiotou, C. Phase compositions and saturated densities for the binary systems of carbon dioxide with ethanol and dichloromethane. *Fluid Phase Equilib.* **2004**, *224*, 89−96.

Received for review March 4, 2006. Accepted May 12, 2006. We are thankful to EPSRC (Grants GR/R02863 and GR/S87409) and to the Marie Curie Research Training Network SuperGreenChem (MRTN-CT-2003-504005) for financial support.

JE060099A